Ramifications of Pulsed Laser Deposition Growth Temperature on BaHfO₃ and Y₂O₃ Doped Y-Ba-Cu-O Thin Films' Microstructure and Performance

M. A. Sebastian, C. R. Ebbing, Han Wang, Haiyan Wang, B. Gautam, J. Z. Wu, T. J. Haugan

Abstract— Deposition temperature is an important parameter to control in pulsed laser deposition of thin films, as it affects the adatom mobility and diffusion in regards to film growth. Increased growth temperature can also result in increased stacking fault densities in YBa₂Cu₃O_{7- δ} (YBCO) films. This research investigates the influence of deposition temperature on the critical current density and the microstructure of YBCO thin films double doped with BaHfO₃ and Y₂O₃. A KrF excimer laser was used to produce thin films of YBCO doped with 4 vol. % BaHfO₃ and 3 vol. % Y₂O₃ on LaAlO₃ (LAO) substrates at various deposition temperatures from 790–825 °C. The growth temperature influence on the flux pinning landscape and J_c (H, T, θ) properties (T = 5-77 K, H = 0-9 T, $\theta = 0-180$ °) of these films will be presented.

Index Terms—Critical current density, flux pinning, hafnium compounds, superconducting thin films, yttrium barium copper oxide

I. Introduction

PREVIOUS research confirmed that the BaHfO₃ (BHO) one dimensional artificial pinning centers (1D APCs) can be best tuned by the addition of secondary Y_2O_3 three dimensional (3D) APCs, leading to a different pinning landscape [1]–[9]. The quality and microstructure of films grown by pulsed laser deposition is dependent on many variables, such as: the laser energy and repetition rate, chamber atmosphere, the heater block temperature, and the choice of substrate [9]–[13]. In this paper, we investigate the growth temperature (T_g)

Manuscript received on Oct_ 2020 and accepted on_2021. This work was supported by AFRL/ Aerospace Systems Directorate and the Air Force Office of Scientific Research (LRIR No. 14RQ08COR and No. 18RQCOR100), and by National Science Foundation DMR-1565822 & DMR-2016453 for TEM courtesy of H. Wang's research group, and NSF contracts Nos. NSF-DMR-1909292 and NSF-DMR-1508494 for angular current density measurements courtesy of J. Wu's research group.

(Corresponding author: Mary Ann Sebastian.)

M. A. Sebastian & C. R. Ebbing are with the University of Dayton Research Institute, Dayton, OH 45469, USA (e-mail: mary_ann.sebastian.l.ctr@us.af.mil, charles.ebbing.ctr@us.af.mil).

Timothy J. Haugan is with the Air Force Research Laboratory RQQM, Wright Patterson AFB, OH 45433 USA (e-mail: timothy.haugan@us.af.mil).

J. Z. Wu (jwu@ku.edu) is with the Dept. of Physics and Astronomy, University of Kansas, Lawrence, KS 66045 USA (e-mail: jwu@ku.edu, B. Gautam was with the University of Kansas, and is now with Intel, Hillsboro, OR 97123 USA (email: gautambik@gmail.com)

Haiyan Wang is with the School of Materials Engineering, Purdue University, West Lafayette, IN 47907 USA (e-mail: hwang00@purdue.edu). Han Wang was with Purdue University and is now with PNNL, Richland, WA 99354, USA (email: han.wang@pnnl.gov).

Color versions of one or more of the figures in this paper are available online at http://ieeexplore.ieee.org. Digital Object Identifier inserted here.

effect on BHO 1D APCs by quantitative evaluation of electrical transport $J_c(H,T,\theta)$ measurement and microstructure observation in 4 vol. % BHO + 3 vol. % Y_2O_3 nanocomposite films deposited on LAO substrate at 790 °C–825 °C. We have found that the pinning ability and pinning strength quantitatively expressed as pinning force density (F_p), and maximum field (H_{max}) of the APCs is increased with T_g at its optimum growth temperature. These values are lower when films are grown either below or above the optimal growth temperature of the 4 % BHO double doped (DD) thin films which could be possible either by insufficient crystallinity of 1D APCs during film growth or by incoherent APC/YBCO interface. These arguments are supported by the microstructure observed in the TEM images.

II. EXPERIMENTAL

A. Thin Film Production

Three sets of thin films were produced via pulsed laser deposition from a mixed YBCO target consisting of 4 vol. % BaHfO₃ and 3 vol. % Y₂O₃, with the remaining percentage consisting of YBCO. A Lambda Physik LPX 300 KrF excimer laser (248 nm) was utilized for the depositions at a fluence of approximately 1.6 J/cm² and a repetition frequency of 8.0 Hz. Films were fabricated at the growth temperature of 790 °C–825 °C at an oxygen partial pressure of 300 mTorr on (100) LaAlO₃ (LAO) single crystal substrates. All samples were further annealed at 500 °C for 30 minutes approximately at one atmosphere oxygen pressure. The film thicknesses were determined using a K-16 Tencor profilometer, and range from 160–190 nm.

B. Thin Film Characterization

For electrical transport measurements, two parallel microbridges of length 500 μ m, and width of 20 μ m and 40 μ m, respectively, were patterned using a standard photolithography technique. The electrical transport J_c (H, T, θ) as a function of temperature T, magnetic field H and critical temperature T_c were determined using the Quantum Design Ever-Cool II Physical Properties Measurement System (PPMS) and a vibrating sample magnetometer (VSM) respectively. A Keithley 2430 1 kW pulsed current source meter and HP 34420 were employed to measure the current-voltage (I-V) characteristics,

with J_c calculated by utilizing the standard 1 μ V/cm criterion. Magnetic current density measurements were also attained utilizing the VSM-PPMS with the magnetic field applied parallel to the c-direction and ramped from 0–9.0 T at temperatures ranging from 77 K–5 K, and employing the Bean model as referenced in previous papers [14]–[16].

Microstructure was examined by using x-ray diffraction and microscopic techniques. A Bruker D8 Discover with a Cu tube (1.5418 Å) and with a high resolution setting at 40 kV and 40 mA was used to conduct 2 Theta—omega scans from 0°—80° and rocking curve scans of the YBCO (005) peak. Transmission electron microscopy (TEM, FEI TALOS T200X) was operated at 200 kV to attain high resolution images. The fast Fourier Transform (FFT) of high-resolution TEM (HRTEM) images were based on the following steps: first, the area of interests was selected in the TEM image, and then the FFT process of the same area was conducted. By selecting and masking the specific diffraction dots in the FFT, the masked FFT was inverted to the fast Fourier filtered images.

III. RESULTS

Fig. 1 shows the results of magnetic current density verses applied field ramped from 0-9.0 T, measured at 65 K, 50 K, and 5 K. for three films produced by ablating a target consisting of 4 vol. % BHO + 3 vol % Y₂O₃ doped YBCO. Each film was deposited on LAO substrates at a different heater block temperature: 790 °C, 810 °C, and 825 °C. The film deposited at 810 °C achieves the highest current density across the board for all fields and temperatures measured. From Table I, it is seen that the critical temperature (T_c) increases with increasing deposition temperature. Fig. 2 compares the $J_c(H)$ curves of the 4 % BHO DD samples measured at 77 K and 65 K, with the applied field orientations of $\theta=0^{\circ}$ (H//c-axis), $\theta=45^{\circ}$, and θ =90° (H//ab-plane). At H//c-axis in Fig. 2(a), the overall higher $J_c(H)$ values are observed for 810 °C BHO film at all fields up to 9.0 T at 77 K and 65 K. This could be due to enhanced correlated pinning by BHO 1D APCs which is also confirmed quantitatively by the low a value obtained from fitting $J_c(H) \propto H^{-\alpha}$, as compared to $\alpha \sim 0.5$ for the undoped YBCO [17] and to higher α values for films grown at different T_g , as seen in Table II. While the T_c effect cannot be ruled out for the lower $J_c(H)$ measured at 77 K, it is negligible when $J_{\rm c}(H)$ is measured at 65 K. Although $T_{\rm c}$ effect could be reflected more on 790 °C film ($T_c \sim 86.7$ K) compared to the 825 °C film ($T_c \sim 89.3$ K) when measured at 77 K, an increasing gap of $J_c(H)$ beyond 0.7 T indicates that the latter could have strong pinning by 1D APCs. The $J_c(H)$ curves follow the similar trend for the H at θ =45 ° and H//ab-plane on all these films at 77 K and 65 K with overall higher $J_c(H)$ values for 810 °C BHO film. The same $\alpha \sim 0.26$ value when H//ab-plane indicates similar pinning behavior by APCs along ab-plane in these films. Comparably lower $\alpha \sim 0.23$ and 0.24 values when H at θ =45 ° and H//ab-plane for 810 °C BHO film is an indication of comparatively strong pinning. It means the most probable explanation for the slightly lower $J_c(H)$ in the 790 °C and

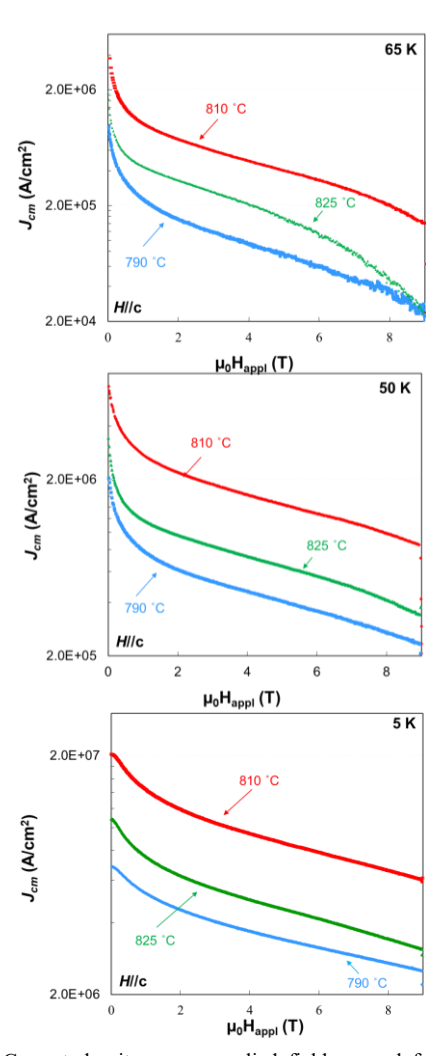


Fig. 1. Current density verses applied field ramped from 0– $9.0\,\mathrm{T}$ at 65 K, 50 K, & 5 K. Each curve corresponds to a film deposited at a different substrate PLD temperature, as marked in the graphs.

TABLE I
CRITICAL TEMPERATURES FOR YBCO & BHO DD YBCO FILMS
DEPOSITED AT VARIOUS DEPOSITION TEMPERATURES

Film	YBCO	4 % E	BHO + 3 %	Y ₂ O ₃
Deposition Temp. (°C)	790	790	810	825
$T_{c}\left(\mathbf{K}\right)$	89.2	86.66	88.82	89.31

 $TABLE\ II$ $F_{PMAX}, H_{MAX}, \&\ ALPHA\ VALUES\ FOR\ BHO\ DD\ YBCO\ FILMS\ DEPOSITED\ AT$ $VARIOUS\ DEPOSITION\ TEMPERATURES$

Depos	sition		77 K			65 K	
T (°C	2)	Н∥с	H	H ab	Н∥с	H	H ab
			⊖=45°			⊖=45°	
790	F _{pmax}	0.54	0.67	2.56	31.13	18.06	24.8
	(GN/m^3)						
	$H_{max}(T)$	0.7	1.0	2.0	9.0	6.0	6.5
	α	0.48	0.45	0.36	0.24	0.26	0.264
810	$F_{p max}$	7.36	5.66	9.07	67.72	45.25	54.16
	(GN/m^3)						
	$H_{max}(T)$	4.0	2.5	4.0	7.5	8.5	9.0*
	α	0.35	0.40	0.34	0.13	0.23	0.24
825	F _{p max}	2.51	2.24	4.98	28.01	18.92	25.93
	(GN/m^3)						
	$H_{max}(T)$	3.5	2.5	3.0	8.0	6.50	8.50
	α	0.42	0.42	0.33	0.25	0.29	0.26

^{*}indicates instrument limit

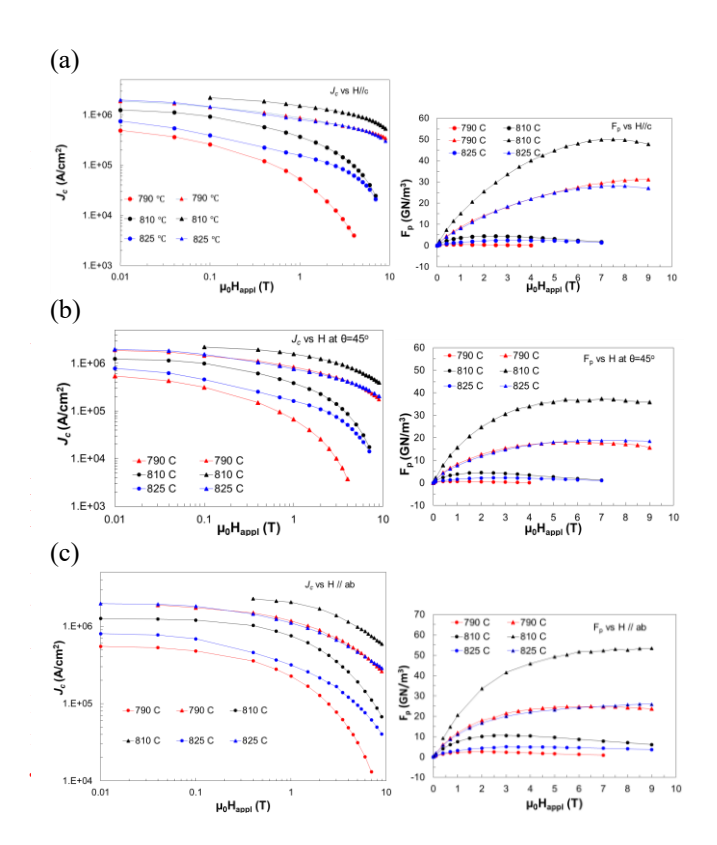


Fig. 2. $J_{\rm c}$ vs H and F_p vs H curves of 4 % BHO DD samples measured at the field orientation of (a) θ =0 ° (H//c-axis), (b) H at θ =45 °, and (c) θ =90 ° (H//ab-plane), and at temperatures of 77 K (circle) and 65 K (triangle) respectively. Color codes follow the same for all samples as 790 °C (red), 810 °C (black) and 825 °C (blue).

825 °C BHO films compared to the 810 °C BHO DD film could be slightly more disturbance of film matrix along *ab*-plane. The effectively longer length of the 1D APCs and larger 3D APCs along with less disturbance of *ab*-plane in the latter may provide more effective pinning results and overall higher $J_c(H)$ in all field orientations. We may argue that the growth temperature affects the kinetic diffusion process during the BHO 1D APCs formation as well as the strain at APC/YBCO interface.

Fig. 2(a–c) also compares the pinning force density $(F_p=J_c \times J_c)$ H) calculated from the $J_c(H)$ curves as a function of the field H at orientations of θ =0°, 45° and 90°, measured at 77 K and 65 K. At H//c-axis, the typical bell shaped $F_p(H)$ curve with the highest $F_{p,max}$ values at the matching field H_{max} for 810 °C BHO DD film in fact leads the highest $J_c(H)$ values in Fig. 2(a-c). At H//c-axis, the $F_{p,max} \sim 68 \text{ GN/m}^3$ is more than two times higher than $F_{p,\text{max}} \sim 31 \text{ GN/m}^3$ and $\sim 28 \text{ GN/m}^3$ the H_{max} for 790 °C and 825 °C films at 65 K where the T_c effect is negligible, and indicates the strong correlated pinning by BHO 1D APCs aligned in the c-axis. At H//c-axis, the comparable H_{max} values for all films (Table II) but higher $F_{\text{p,max}}$ values for the 810 °C BHO DD film could be due to the effectively longer length of the c-axis aligned BHO 1D-APCs with comparably equal areal density in latter ones. Similarly, the higher $F_{\rm p,max}$ observed at H at θ =45 ° and H//ab-plane for this film at 77 K and 65 K indicates the strong pinning by randomly distributed 3D APCs, and 1D APCs aligned along ab-plane re-

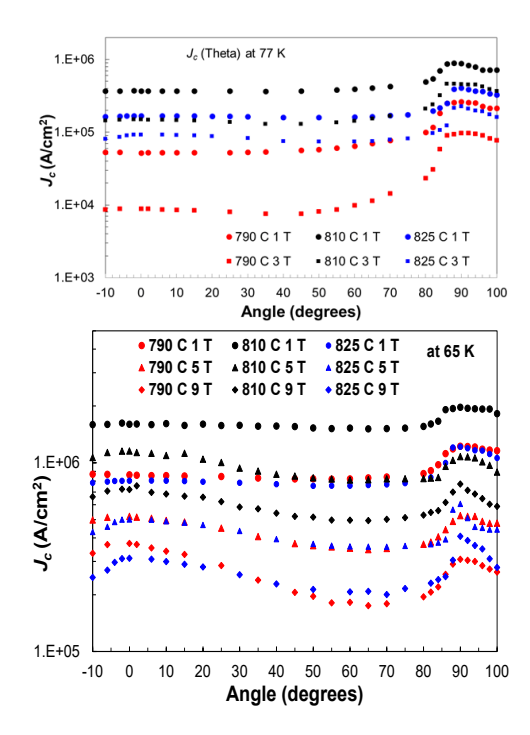


Fig. 3. Angular transport current density at 77 K & 65 K with the field applied at different angles with respect to the film surface: H//c at 0 ° and H//ab at 90 °.

spectively. It further implies that BHO 1D APCs are possibly the dominant pinning centers instead of Y₂O₃ 3D APCs in the 810 °C BHO DD film. The similar trend of $F_{p,max}$ and H_{max} are observed for 790 °C and 825 °C BHO DD films with H at θ =45° and H//ab-plane as shown in Fig. 2(b, c). Although slightly higher $F_{p,\text{max}} \sim 2.24 \text{ GN/m}^3$ and 4.98 GN/m^3 and H_{max} ~2.4 T and 3.0 T are observed for latter film at 77 K, while comparable $F_{p,max}$ and H_{max} values are observed at 65 K (Table II) at the field orientation of θ =45 ° and H//ab-plane respectively. It means at growth temperatures ~ 790 °C and 825 °C, there could be subtle difference of APCs morphology and orientation in BHO DD films. There could be a similar effect of APCs microstructure on the ab-plane of film matrix as well. However, the higher $F_{p,max}$ with comparatively similar H_{max} for 810 °C film compared to other two films, could be from difference of effective length as well as the APC/YBCO interface having comparatively similar effective number density of APCs.

Fig. 3 examines the angular transport current density measured at 77 K, 1 T and 3 T and at 65 K for 1 T, 5 T and 9 T, for each of these films. At 77 K, J_c peaks at H//c-axis are not clearly seen while appearance of J_c peak at H//ab-plane indicates strong intrinsic pinning. At 65 K, the J_c valleys are observed because of weaker pinning and J_c peaks at H//c-axis at 5.0 T and 9.0 T while such valleys are absent for 1.0 T due to much lower field compared to matching field. At 1.0 T, the J_c s for all three films exhibit negligible variation in a wide θ range of 0–80 °, suggesting the pinning provided by the APCs of mixed morphologies is uniform. The minor J_c peak at θ =90 ° can be attributed to the intrinsic pinning of the CuO₂ planes. With increasing field, a broader J_c peak emerges and at 9.0 T this peak has comparable height to that at θ =90 °. This sug-

gests that the BHO 1D APCs can provide strong correlated pinning comparable to the intrinsic pinning at high fields due to their high accommodation fields. In contrast, Y₂O₃ NPs are effective only at low fields. In comparison, the film grown at the optimal temperature of 810 °C with the larger diameter BHO 1D APCs exhibit stronger pinning efficiencies, which explains the higher overall $J_c(\theta)$ as compared to the counterparts' in the other two films. The appearance of J_c -peaks at H//c-axis further indicates the increasing vortex pinning by APCs with decreasing temperature. The presence of J_c valley leads to increase J_c -anisotropy: mathematically calculated $(J_{c,max} - J_{c,min})/J_{c,min}$ where $J_{c,max}$ is the crest and $J_{c,min}$ is the trough of $J_c(\theta)$ curve for the angular range from $\theta=0$ °-90 °. Smaller J_c -anistropy indicates stronger isotropic pinning. The J_c anisotropy of 1.53 at 3.0 T and 77 K for 810 °C BHO DD film is lower than the J_c -anisotropy 1.54 for 790 °C and 2.04 for 825 °C BHO DD film at the same field and temperature, which indicates stronger pinning in the former. Similarly, at 65 K, the lower J_c anisotropy is obtained at 5.0 T and 9.0 T for the 810 °C BHO DD film compared to other two films (Table III). At 65 K, smaller J_c -anisotropy for lower T_g 790 °C film at the field of 5.0 T, and smaller J_c -anisotropy for T_g 825 °C film at the field of 9.0 T indicate that the former has more isotropic pinning at moderate field while the latter has more isotropic pinning at high field. However, the J_c -anisotropy of these films are still larger than the J_c -anisotropy ~ 0.18 of 2 vol. % BHO DD nanocomposite film at 9.0 T and 65 K [2]. These results il-

 ${\it TABLE~III} \\ J_{\it CT}~{\it ANISOTROPY~FOR~4~VOL.\%~BHO~DD~YBCO~FILMS}$

_		Jc anis	sotropy	
Deposition Temp. (°C)	77	′ K	65	K
	1.0 T	3.0 T	5.0 T	9.0 T
790	4.05	1.54	0.51	1.14
810	1.04	1.53	0.42	0.56
825	1.54	2.04	0.69	1.04

lustrate the effect of growth temperature on the generation of the APC morphology and orientation.

XRD analysis in Fig. 4, illustrates very nice epitaxial growth in the c-direction, confirmed with (00l) peaks for the YBCO doped film and the LAO substrate. BHO and Y_2O_3 peaks are also apparent. Analysis of the rocking curve scans on the YBCO (005) peaks in the inset of Fig. 4 and Table IV show that the peak shifts right and the FWHM decreases as the deposition growth temperature increases. This correlates with a larger c-lattice length and larger grain size respectively.

The high-resolution TEM (HRTEM) images in Fig. 5(a–c) shows BHO nanorods, and the corresponding fast Fourier transform (FFT) analysis Fig. 5(d–f) shows that the stalking faults density increases with increasing growth temperature. Another interesting phenomenon presented by the TEM images is that the 810 °C sample has the smaller lateral dimensions of the YBCO nanopillars and larger BHO nanopillars than the other two samples, as seen in Table V. The BHO nanopillars also have a lower density in the 810 °C sample, which may re-

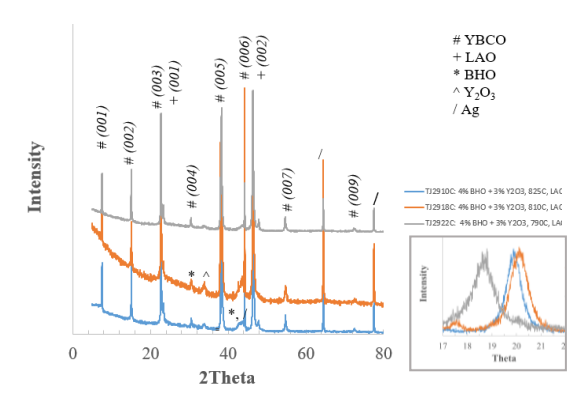


Fig. 4. X-ray diffraction 2Theta-omega scans of the analyzed films with rocking curve scans YBCO (005) displayed in the inset.

 $\label{eq:table_iv} \textbf{TABLE IV} \\ \textbf{XRD ANALYSIS FOR 4 VOL. \% BHO DD YBCO FILMS} \\$

Deposition Temp. (°C)	YBCO (005) FWHM	YBCO (005) c-lattice (Å)
790	0.770	11.7373
810 825	0.770 0.676	11.7147 11.7157

YBCO c-lattice parameter = 11.707 Å thin film & 11.66 Å for a single crystal.

sult in the strong and isotropic pinning performance. The HADDF image of the 810 °C sample and the corresponding EDS mapping data confirms the presence of BHO nanorods and Y₂O₃ nanoparticles. This impact of the size of the BHO nanorods on pinning efficiency due to the resulting strain fields and microstructure defects is similar to results found in regards to the size of BaZrO₃, nanorods in previous research[18].

CONCLUSION

A comparative study has been carried out to probe the effect of the growth temperature on BHO 1D APCs in 4 vol. % BHO DD films. Temperature is an important variable in crystalline growth. Adatom mobility is increased with increasing temperature. This, in turn influences the diffusion of the adatoms, since the diffusivity coefficient is related to temperature in an Arrenhius type of equation [19]. The dimension of APCs microstructure correlates with diffusion of adatoms through growth temperature which in turn affects the APCs morphology to generate the pinning landscape. The transport J_c is measured at the temperature of 65-77 K at the field up to 9.0 T at different orientations and the APCs microstructures are observed in the TEM images. The optimum growth temperature of 810 °C is obtained for 4 vol. % BHO DD films to generate the overall strong and more isotropic pinning at 77 K and 65 K which correlates with TEM microstructures. For low growth temperature of 790 °C film, more isotropic pinning at moderate field of 5.0 T and less isotropic pinning at high field of 9.0 T is observed compared to high growth temperature 825 °C film at same field and at 65 K. The results of this research is relevant to future applications for superconducting wire use in magnets [20].

TABLE III	
TEM ANALYSIS	5

Deposition Temp. (°C)	D _{YBCO} (nm)	D _{BHO} (nm)
790	8.3 ± 1.4	3.3 ± 0.6
810 825	4.6 ± 2.2 8.0 ± 1.9	3.8 ± 1.0 3.4 ± 0.4

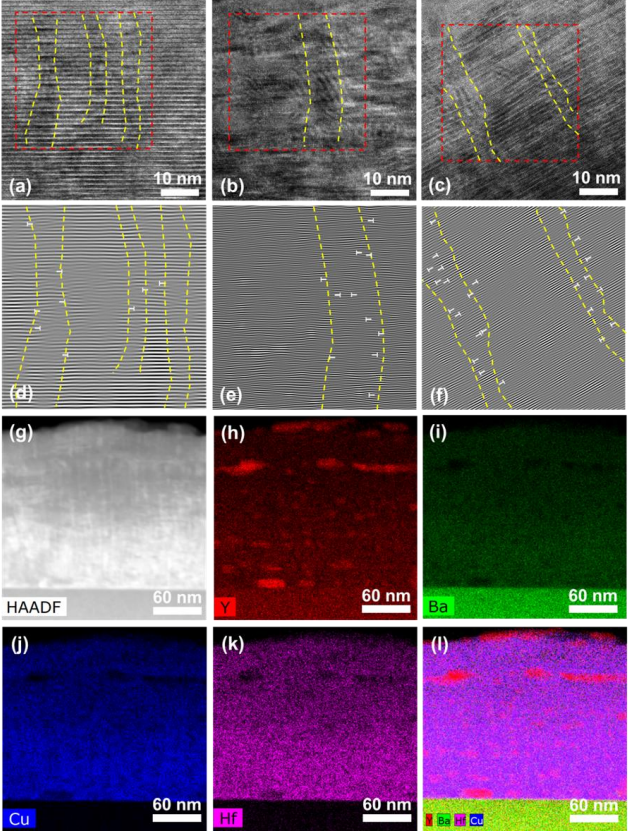


Fig. 5 HRTEM images of 4 % BHO DD films at T_g of (a) 790 °C, (b) 810 °C, and (c) 825 °C. The corresponding fast Fourier filtered images (d–f) of the marked area (red rectangles). HADDF image of the 4 % BHO DD film at T_g of 810 °C and the corresponding EDS analysis for Y, Ba, Cu, and Hf (g–k).

REFERENCES

- [1] M. A. Sebastian, B. Gautam, C. R. Ebbing, G. Y. Panasyuk, M. A. Susner, J. Huang, W. Zhang, H, Wang, J. Z. Wu, T. J. Haugan, "Comparison study of the flux pinning enhancement of YBa₂Cu₃O₇₋₈ thin films with BaHfO₃ + Y₂O₃ single and mixed phase additions," *IEEE Trans. Appl. Supercond.*, vol. 29, no. 5, Jan. 2019, Art. no. 8002005.
- [2] B. Gautam, M. A. Sebastian, S. Chen, J. Shi, T. Haugan, Z. Xing, W. Zhang, J. Huang, H. Wang, M. Osofsky, J. Prestigiacomo, J. Z. Wu, "Transformational dynamics of BZO and BHO nanorods imposed by Y₂O₃ nanoparticles for improved isotropic pinning in YBa₂Cu₃O_{7-δ} thin films," AIP Adv., vol. 7, no. 7, Jul. 2017, Art. no. 7,075308.
- [3] B. Gautam, M.A Sebastian, S. Chen, T. Haugan, W. Zhang, J. Huang, H. Wang, J. Z. Wu, "Microscopic adaptation of BaHfO₃ and Y₂O₃ artificial pinning centers for strong and isotropic pinning landscape in

- YBa₂Cu₃O_{7-x} thin films," Supercond. Sci. Tech., vol. 31, no. 2, Jan. 2018, Art. no. 025008
- [4] M. Sieger, P. Pahlke, M. Lao, A. Meledin, M. Eisterer, G. Van Tendeloo, et al., "Thick secondary phase pinning-enhanced YBCO films on technical templates," *IEEE Trans. Appl. Supercond.*, Jun. 2018, vol. 28, no 4, Art. no. 8000505.
- [5] S. Sato, T. Honma, S. Takahashi, K. Sato, M. Watanabe, K. Ichikawa, et al., "Introducing artificial pinning centers into YBCO thin films to improve surface resistance in a DC magnetic field," *IEEE Trans. Appl. Supercond.*, vol. 23, no. 3, Jun. 2013, Art no. 7200404.
- [6] M. Watanebe, S. Sato, K. Sato, K. Ichikawa, A. Saito, S. Ohshima, "Experimental study in the development of HTS NMR probe," 11th European Conference on Applied Superconductivity, Genoa, Italy, Sept. 2013, J. Phys. Conf. Ser, vol. 507, part 1, 2014.
- [7] M. Sieger, J. Hanisch, P. Pahlke, M. Sparing, U. Gaitzsch, K. Iida, et al., "BaHfO₃-doped thick YBa₂Cu₃O_{7.5} films on highly alloyed textured Ni-W tapes," *IEEE Trans. Appl. Supercond.* Vol. 25, no. 3, Jun. 2015, Art no. 6602604.
- [8] T. Matsushita, H. Nagamizu, K. Tanabe, M. Kiuchi, E. Otabe, H. Tobita, et al., "Improvement of flux pinning performance at high magnetic fields in GdBa₂Cu₃O_y coated conductors with BHO nano-rods through enhancement of B_{c2}," Supercond. Sci. Technol., vol. 25, no. 12, Oct. 2012, Art no. 125003.
- [9] D. M. Feldmann, O. Ugurlu, B. Maiorov, L. Stan, T. G. Holesinger et al., "Influence of growth temperature on critical current and magnetic flux pinning structures in YBa₂Cu₃O_{7-x}," Appl. Phys. Lett., vol. 91, no. 16, Oct.2007, Art. no. 162501.
- [10] J. Wang, J. H. Kwon, J. Woon, H. Wang, T. J. Haugan, F. J. Baca, et al., "Flux pinning in YBa₂Cu₃O_{7-δ} thin film samples linked to stacking fault density," Appl. Phys. Lett., vol. 92, no. 8, Feb.2008, Art. no. 082507
- [11] M. A. Sebastian, J. N. Reichart, M. M. Ratcliff, T. J. Bullard, J. L Burke, C. R. Ebbing, et al., "Study of the flux pinning landscape of YBCO thin films with single and mixed phase additions BaMO₃+ Z: M = Hf, Sn, Zr and Z=Y₂O₃, Y211," *IEEE Trans. Appl. Supercond.*, vol. 27, no. 4, Jun. 2017, Art. no. 7500805.
- [12] T. Horide, K. Torigoe, R. Kita, R. Nakamura, M. Ishimaru, S. Awaji, et al., "Deposition temperature dependence of vortex pinning property in YBa₂Cu₃O₇ + BaHfO₃ Films," *Mater. Trans.*, vol. 61, no. 3, Mar. 2020, pp.449–54.
- [13] M. Ohring, Materials Science of Thin Films, 2nd ed. San Diego, CA: Academic Press; 2002
- [14] J. Kell, T. Haugan, M. Locke, P. Barnes, "Tb and Ce doped Y123 films processed by pulsed laser deposition," *IEEE Trans. on Appl. Supercond.*, vol. 15, no. 2, Jun. 2005, pp.3726–3729.
- [15] C. Bean, "Magnetization of hard superconductors," Phys. Rev. Lett., vol. 8, no. 6, Mar. 1962, pp. 250–253.
- [16] C. Bean, "Magnetization of high field superconductors," Rev. Mod. Phys., vol. 36, Jan. 1964, pp. 31–39.
- [17] V. I. Matsui, V. S. Flis, V. O. Moskaliuk, A. L. Kasatkin, N. A. Skoryk, V. L. Svechnikov, "Current-carrying abilities of nano-structured HTS thin films," *J. Nanosci. and Nanoeng.*, vol. 1, no. 2, 2015, pp. 38–43.
- [18] V. Ogunjimi, B. Gautam, M. A. Sebastian, T. J. Haugan, J. Z. Wu, "The one-dimensional artificial pinning centers in BaZrO₃/YBa₂Cu₃O_{7-x} nanocomposite films," AIP Adv, vol. 9, no. 8, Aug. 2019, Art. no. 085110.
- [19] W. Callister, W. Wright, The Science and Engineering of Materials, 5th edition, Cengage Learning, USA 2017
- [20] J. P. F. Feighan, A. Kursumovic, J. L. MacManus-Driscoll, "Materials design for artificial pinning centres in superconductor PLD coated conductors," *Supercond. Sci. Technol.*, vol. 30, no. 12, Nov. 2017, Art. no. 123001.